Abdominal Radiology (2019) 44:2329–2336
https://doi.org/10.1007/s00261-019-01973-w

HOLLOW ORGAN GI

Gastrointestinal stromal tumor risk classification: spectral CT quantitative parameters

Xueling Zhang[1] · Liangcai Bai[1] · Dan Wang[1] · Xiaoyu Huang[1] · Jinyan Wei[1] · Wenjuan Zhang[1] · Zhuoli Zhang[2] · Junlin Zhou[1,3]

Published online: 12 April 2019

Abstract

Purpose To examine the value of spectral CT quantitative parameters in gastrointestinal stromal tumor (GIST) risk classification.

Materials and methods This retrospective study was approved by the institutional review board. The requirement for informed consent was signed. The authors evaluated 86 patients (30 high risk, 22 medium risk, 28 low risk, and 6 very low risk; mean age: 59 years [range 19–83 years]) with pathologically confirmed GIST who underwent plain and triple-phase contrast-enhanced CT with spectral CT imaging mode from March 2015 through September 2017, with manual follow-up. Quantitative parameters including the CT value of 70 keV monochromatic images, the slope of spectral curves, and the normalized iodine concentration (NIC) and water (iodine) concentrations were measured and calculated, and conducted a power analysis of the above data.

Results (1) The CT values at 70 keV of the high-risk group were higher than the intermediate and low groups in each of the enhanced phases ($P \leq 0.001$), no significant differences in the intermediate-risk and low-risk groups were noted ($P = 0.874$, 0.871, 0.831, respectively). (2) The slope of the spectral curve of the high-risk group was higher than those of the intermediate and low groups in each of the enhanced phases ($P \leq 0.001$), and there were no significant differences between the intermediate- and low-risk groups ($P = 0.069$, 0.466, 0.840, respectively). (3) The NIC of the high-risk group significantly differed from the lower risk groups ($P \leq 0.001$). There was also no significant difference observed between the intermediate- and low-risk groups ($P = 0.671$, 0.457, 0.833, respectively). (4) The power analysis results show that only the low-risk group with delay period is 0.530, the rest groups are all greater than 0.999.

Conclusion Dual-energy spectral CT with quantitative analysis may help to increase the accuracy in differentiating the pathological risk classification of GIST between high risk and non-high risk, preoperatively. There were limitations for distinguishing the intermediate- and low-risk groups.

Keywords Gastrointestinal stromal tumor · Spectral CT · Quantitative parameters · Risk classification

Introduction

The GIST recurrence risk stratification criteria, which is currently recognized and widely used internationally, is recommended by the National Institutes of Health (revised in 2008) and can be divided into high, intermediate, low and very low risk based on tumor size, mitotic index, primary site, and tumor rupture [1]. Then higher risk corresponds to higher recurrence and mortality [2, 3]. Thus, preoperative examination to assess the risk rating is essential.

Imaging examination is the main method of GIST diagnosis, differential diagnosis, and preoperative assessment, and CT imaging is the main method of comprehensive

✉ Junlin Zhou
LZUzjl601@163.com

[1] Department of Radiology, Lanzhou University Second Hospital, Lanzhou 730030, People's Republic of China

[2] Department of Radiology, Northwestern University, Chicago, IL 60611, USA

[3] 82# Cuiyingmen, Chengguan District, Lanzhou, Gansu, People's Republic of China

assessment of gastrointestinal lesions prior to surgery [4, 5]. Compared with the traditional CT, the gemstone spectral CT used in this study has the advantage of multiple parameters, such as the monochromatic image CT value, the slope of the spectral curve, and the iodine concentration, which have been used in gastric cancer staging evaluation [6]. The purpose of this study was to investigate the feasibility of using the above spectral CT quantitative parameters for GIST risk classification.

Materials and methods

Patients and setting

The Ethics Committee at our Hospital approved this retrospective study, and all patients provided their written informed consent. Our radiology database from March 2015 to September 2017 was screened for patients with GIST who had serial imaging studies available for review, in which 199 patients were identified. All of them underwent nonenhanced CT and triple-phase contrast-enhanced CT. Of the 199 identified patients, 113 patients were excluded because they were scanned with the conventional scanning mode rather than the dual-energy spectral mode. Thus, the final study cohort included 86 patients(44 men, 42 women; mean age ± standard deviation, 57 years ± 13; age range 19–83 years).All 86 patients were confirmed to have GIST by surgical and pathological assessment and were divided into three groups based on the National Institutes of Health criteria, high risk (20 men, 10 women; mean age, 59 years ± 15; age range 19–83 years), medium risk (10 men, 12 women; mean age, 57 years ± 13; age range 23–72 years), low and very low risk for the same team in the study(11 men, 23 women; mean

Table 1 General information of patients

Characteristics	No. of patients
Age(y)	
≤ 40	8(9.3)
> 40 to ≤ 65	52(60.5)
> 65	26(30.2)
Sex	
Male	44(51.2)
Female	42(48.8)
Location of GIST	
Stomach	61(70.9)
Duodenum	7(8.1)
Small bowel	13(15.2)
Colon and anorectal	5(5.8)
Growth pattern	
Intracavity	47(54.7)
Out of cavity	27(31.4)
Inside and outside	12(13.9)
Size of the primary tumor (cm)	
≤ 2	11(12.8)
> 2 to ≤ 5	35(40.7)
> 5 to ≤ 10	26(30.2)
> 10	14(16.3)
Risk stratification	
Very low	6(7.0)
Low	28(32.6)
Intermediate	22(25.6)
High	30(34.8)

Data in parentheses are percentages

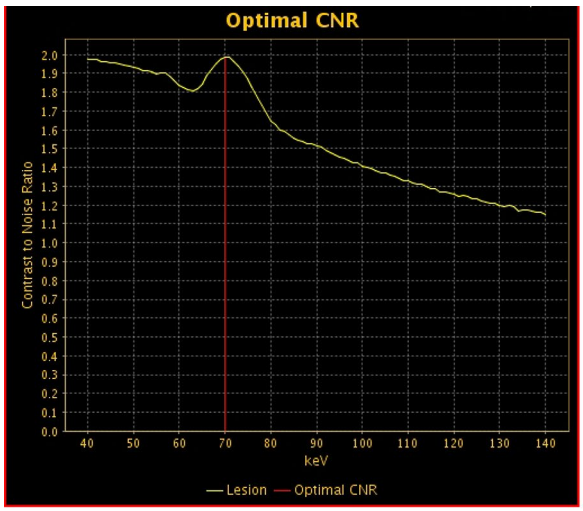

A

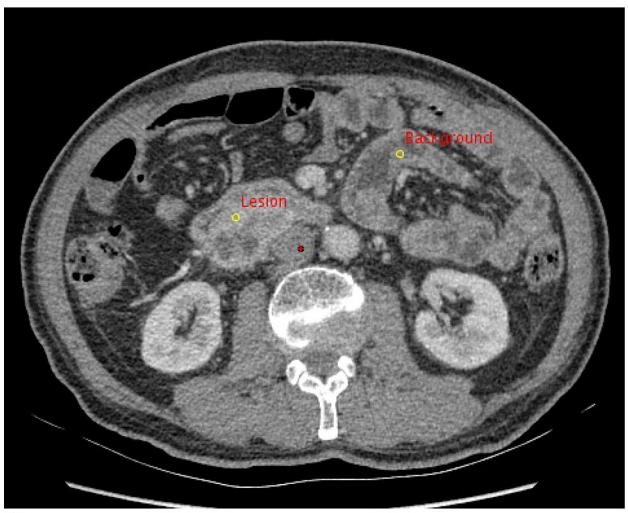

B

Fig. 1 Selecting the best contrast-to-noise ratio (CNR) for displaying GIST with GSI Viewer analysis tool. Optimal monochromatic energy of 70 keV achieved the best CNR for the primary lesion (**a**). ROI selections for primary lesion and normal intestinal wall on an axial image (**b**)

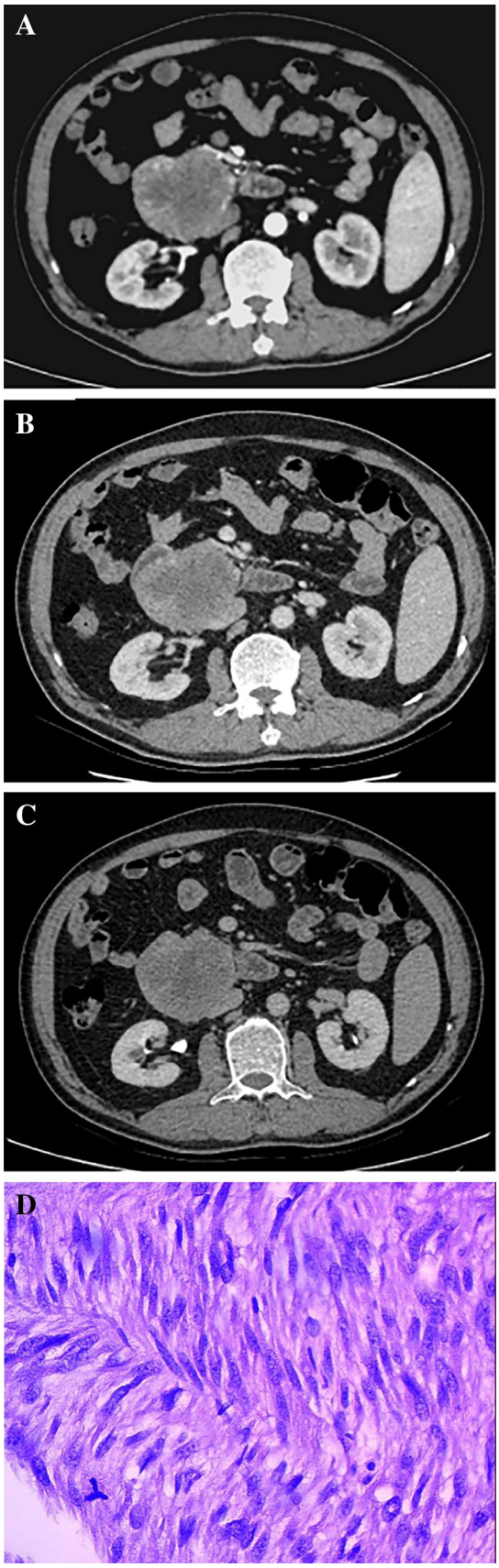

Fig. 2 A 70-year-old male with high-risk GIST in the duodenum. ▶ The enhanced CT images revealed an irregular mass in the duodenum descending segment. The lesion exhibited circular significant enhancement in AP, PP, and DP (**a**–**c**). **d** HE staining (×400). The tumor cells were arranged in a matting pattern. Nucleus enlargement, deep staining, with mitosis

age, 54 years ± 11; age range 36–78 years).Additional characteristics are summarized in Table 1.

CT examination

Triple-phase contrast-enhanced CT was performed using a Discovery CT750 HD CT system (GE Healthcare, Waukesha, WI, USA) with the abdomen and pelvis protocol, whose scan range included the superior border of the liver up to the upper edge of the pubic symphysis. Nonenhanced images were acquired using the conventional helical scan mode at 120 kVp tube voltage. The patients were then injected with non -ionic contrast medium (iohexol, 300 mg iodine/mL) via antecubital venous access at a rate of 3.5–4.0 mL/s for a total of 80–100 mL (1.2 mL/kg of body weight) during the arterial phase (AP), portal phase (PP), and delayed phase (DP). AP scanning began 20 s after the trigger attenuation threshold (100 HU) achieved the level of the supraceliac abdominal aorta. PP scanning began at a delay of 60 s after AP scanning, and DP began at a delay of 90 s after PP scanning. AP, PP, and DP scanning were performed in spectral imaging mode with fast tube voltage switching between 80 kVp and 140 kVp on adjacent views during a single rotation. Other scanning parameters were as follows: 0.625 mm collimation thickness, 600 mA tube current, 0.6 s rotation speed, 0.983 helical pitch, 1.25 mm reconstruction thickness, and inter-slice spacing. CT images were reconstructed by projection-based material-decomposition software using a standard reconstruction kernel.

Quantitative analysis

All measurements were performed on an advanced workstation (AW4.6, Discovery CT 750 HD, GE Healthcare) equipped with a Gemstone Spectral Imaging (GSI) viewer. Circular or elliptical regions of interests (ROI) with an area of approximately 80 mm^2 were marked on the lesions and aorta with a default of 70 keV for monochromatic images (Fig. 1). The ROIs encompassed as much of the enhanced areas of the lesions as possible. Areas containing necrosis, calcification, and large vessels were carefully avoided. To ensure consistency, all measurements were performed by the same researcher for three times at different image levels, and average values were calculated. For all measurements, the size, shape, and position of the ROIs were maintained consistently between the three phases. The GSI Viewer

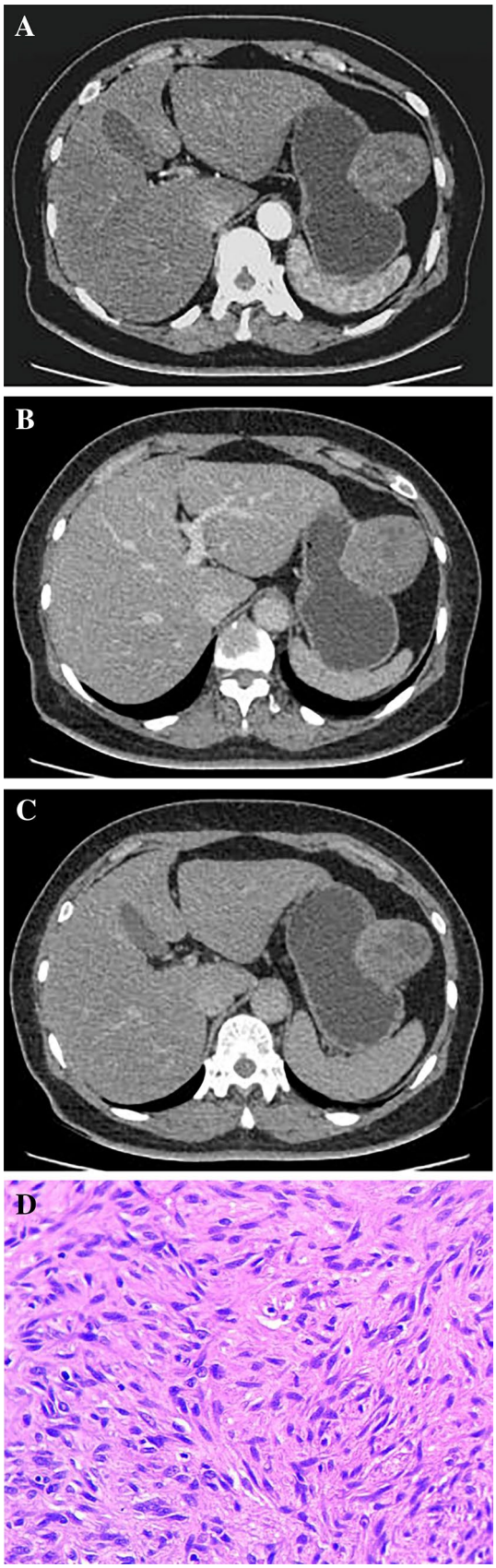

Fig. 3 A 54-year-old female with intermediate-risk GIST in the stomach. The enhanced CT images revealed a circular mass in the greater curvature of the stomach. The lesion exhibited inhomogeneous enhancement in AP, PP, and DP (**a**–**c**). **d** HE staining (×200). The spindle tumor cells were arranged in braiding with an oval nucleus

software automatically calculated the CT attenuation values and iodine (water), and water (iodine) concentrations for the lesions and aorta. Two recently introduced parameters were derived from the iodine concentration measurements and monochromatic images: (a) the normalized iodine concentration (NIC) was calculated as NIC = IClesion/ICaorta, where IClesion and ICaorta are the iodine levels in the lesions and aorta at the same slice, and the iodine concentrations in the lesions were normalized to those of the aorta to minimize variations in patients; (b) the slope of the spectral curve was calculated as slope = (CT40 keV − CT70 keV)/30, where CT40 keV and CT70 keV are the CT attenuation values of the tumors on 40 keV and 70 keV monochromatic images, respectively. The imaging features with different risk were presented in the following images (Figs. 2, 3, 4).

Statistical analysis

All analyses were performed using SPSS23.0 (Chicago, IL, USA). Quantitative values were recorded as the mean ± standard deviation. The quantitative data were compared using one-way ANOVA. Multiple comparisons were performed with statistically significant differences (the adjusted inspection level is $\alpha' = \alpha$/comparison times). The inspection level was $\alpha = 0.05$.

Results

CT values of the 70 keV monochromatic image

The CT values of the 70 keV monochromatic image in patients with different pathological risk classification of GIST are shown in Table 2 and Fig. 5, showing that the CT values of the 70 keV monochromatic image of the high-risk group were higher than the intermediate and low groups in each of the enhanced phases, but no significant differences in the intermediate-risk and low-risk groups were observed ($P = 0.874$, 0.871, 0.831, in each phase, respectively).

Slopes of the spectral curves

The slopes of the spectral curves with different risks in different phases are shown in Table 3 and Fig. 6, suggesting that the CT value in the high-risk group in different phases demonstrated the most statistically significant modification. In addition, there were no significant differences between the

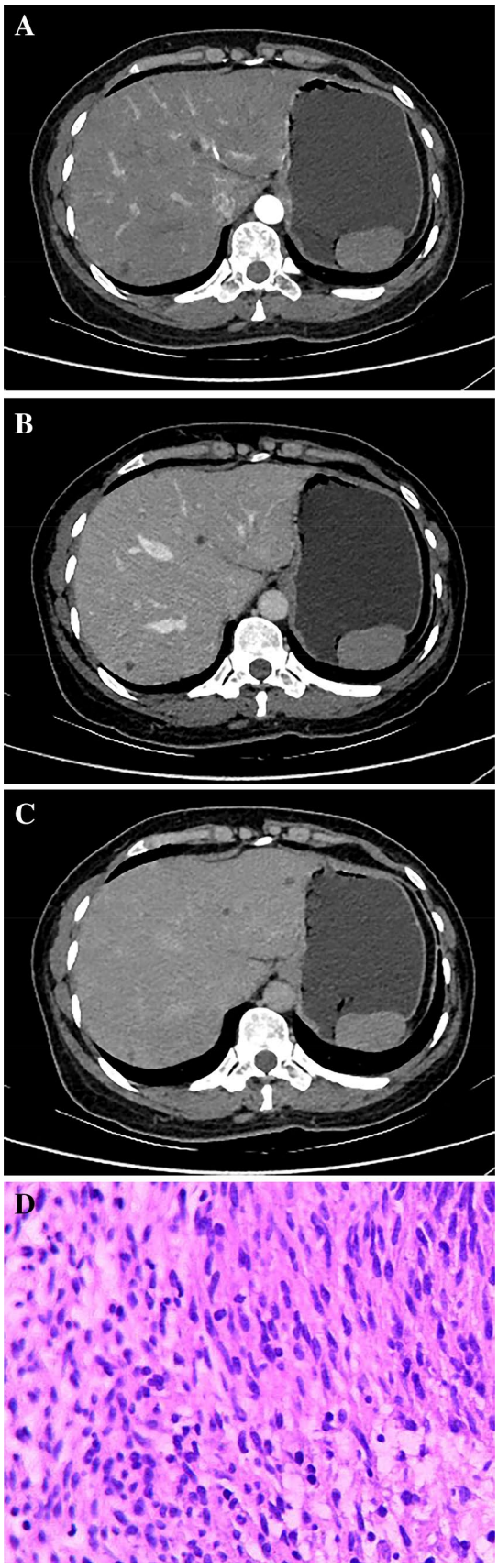

Fig. 4 A 46-year-old female with low-risk GIST in the stomach. The ▶ enhanced CT images revealed an oval mass in the fundus of the stomach. The lesion exhibited mild uniform enhancement (**a**–**c**). **d** HE staining (×200). The spindle tumor cells were arranged in fascicular with rhabditiform nucleus

intermediate- and low-risk groups ($P = 0.069$, 0.466, 0.840, in each phase, respectively).

The normalized iodine concentration (NIC)

The NIC associated with different pathological risk classification of GIST are shown in Table 4 and Fig. 7, indicating a more delayed phase with higher NIC values. There was no statistically significant difference among the WIC values with different risks in different phases ($P = 0.454$, 0.213, 0.115, respectively, Table 4). Statistical analyses also showed that the NIC in patients with high risk significantly differed from patients with lower risk. Furthermore, there was no significant difference between the intermediate- and low-risk groups ($P = 0.671$, 0.457, 0.833, in each phase. respectively).

The power analysis

The power analysis results show that only the low-risk group with delay period is 0.530, the rest groups are all greater than 0.999. The above results may be due to the loss of power due to the nonparametric test method adopted by this group.

Discussion

Currently, several reports have examined imaging for GIST risk classification, but the main methods of introducing quantitative parameters have been MRI and PET/CT [7–9]. Yu et al. [9] performed a comparison of different sized GIST lesions and different degrees of risk with GIST enhancement and diffusion but limited their conclusions to small lesions (less than 5 cm) and found consistent and uniform large lesions (> 5 cm) to display uneven progressive enhancement with cystic degeneration. The rate of tumor cystic degeneration is proportional to the degree of risk [10]. In addition, the correlation analysis between the risk classification and ADC values showed that the ADC value is inversely proportional to the risk. Kamiyama et al. [8] retrospectively analyzed 10 cases (1 male case, 9 female cases) with confirmed GIST using 18F-fluorodeoxyglucose (18F-fluorodeoxyglucose, 18F-FDG) uptake. The mitotic and lesion diameters were examined according to the mitotic index for each of the 50 high-power lenses, and the samples were divided into 2 groups (less than 4 samples per group that is more than 5).

Table 2 The values of the 70 keV monochromatic image with different risk of GIST in different phases

Group	*H*	*I*	*L*	*F/H*	*P*
AP	85.03 ± 14.46	62.37 ± 10.74	65.10 ± 22.43	25.71	< 0.001
PP	88.41 ± 14.66	63.90 ± 10.79	66.22 ± 16.92	24.04	< 0.001
DP	78.36 ± 5.12	66.18 ± 7.16	75.45 ± 22.66	15.30	< 0.001

Table 3 The slope of the spectrum curves with different risks of GIST in different phases

Group	*H*	*I*	*L*	*F/H*	*P*
AP	4.42 ± 1.07	2.27 ± 0.75	2.90 ± 1.61	29.80	< 0.001
PP	4.50 ± 1.35	2.43 ± 0.98	2.63 ± 0.59	36.74	< 0.001
DP	4.20 ± 0.31	2.44 ± 0.81	2.83 ± 0.53	57.42	< 0.001

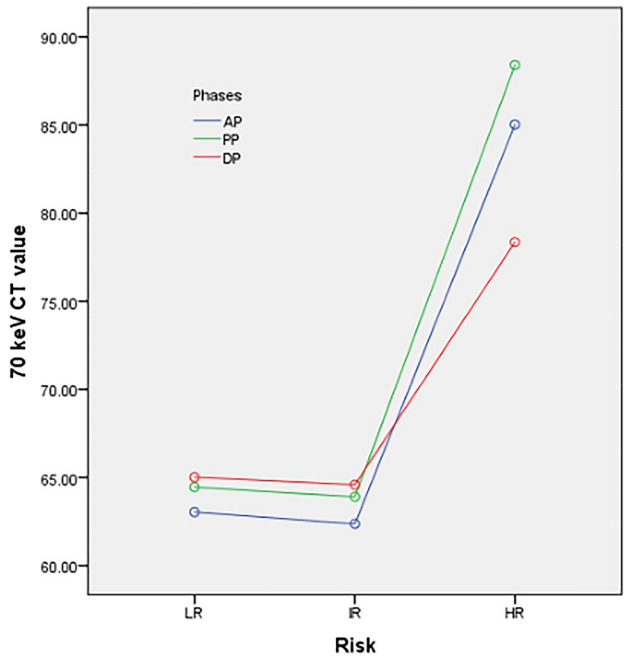

Fig. 5 CT values of the 70 keV monochromatic image with different risk levels in different phases. The CT values of the 70 keV monochromatic image of the high-risk group were higher than the intermediate and low groups in each of the enhanced phases. Note: AP = Arterial phase, PP = Portal phase, DP = Delayed phase, H = High risk, I = Intermediate risk, and L = Low risk

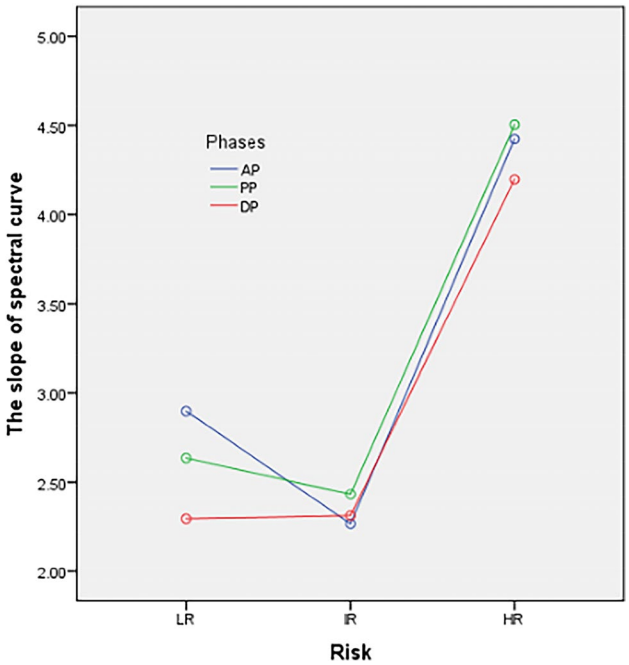

Fig. 6 The slopes of the spectral curves with different risks in different phases. The CT values in the high-risk group in different phases demonstrated the most statistically significant modification

Increased FDG uptake by the lesion was correlated with a higher potential of malignancy. Furthermore, the uptake of FDG was correlated with the Ki-67 index and mitotic values, which could be used as a reliable reference for preoperative evaluation. The present study used CT examination, which is the most convenient and the standard method for abdominal examination and preoperative assessment, and the evaluation of therapy response [11, 12], and the energy spectrum scanning mode was used to obtain quantitative parameters to provide an alternative for preoperative risk classification of GIST.

Our research showed that there were no significant differences in the spectral parameters between the low-risk and intermediate-risk groups in different phases of the enhanced scan. According to the modified NIH criteria [1], it can be inferred that when the tumor size is less than 5 cm (any site of onset) or when the tumor size is approximately 5–10 cm and occurs in the stomach, the change of CT parameters caused by the difference in mitotic values is not sufficient to classify the risk. Therefore, this study combined the intermediate-risk and low-risk groups as a non-high-risk group for discussion. The 70 keV CT value analysis of GIST patients with different risk degrees showed that the CT value of the high-risk group was higher than that of the non-high-risk group in each phase of enhanced scanning. CT enhancement showed marked strengthening. One potential explanation is that a high-risk GIST is more vascular with the increased numbers and larger supplying blood vessels. The endothelial gap increased, and the permeability also increased. The mitotic nuclei are active in high-risk samples. These findings are consistent with the previous literature reports demonstrating the correlation between tumor blood supply types and pathological grade [13–16].

The slope of the spectral curve exhibited significant differences between high-risk and non-high-risk GIST during enhancement phases. The spectral curve reflects

Table 4 The NIC and WIC associated with different risk of GIST in different phases

	Group	*H*	*I*	*L*	*F/H*	*P*
NIC	AP	0.22 ± 0.06	0.11 ± 0.04	0.10 ± 0.05	53.06	< 0.001
	PP	0.78 ± 0.21	0.37 ± 0.11	0.41 ± 0.19	40.45	< 0.001
	DP	1.30 ± 0.10	0.52 ± 0.09	0.64 ± 0.22	59.29	< 0.001
WIC	AP	1025.56 ± 3.96	1025.92 ± 3.93	1026.70 ± 3.15	0.80	0.45
	PP	1026.16 ± 3.32	1025.55 ± 4.04	1027.12 ± 2.87	2.49	0.21
	DP	1.25.00 ± 3.03	1025.10 ± 3.46	1026.46 ± 2.77	2.22	0.12

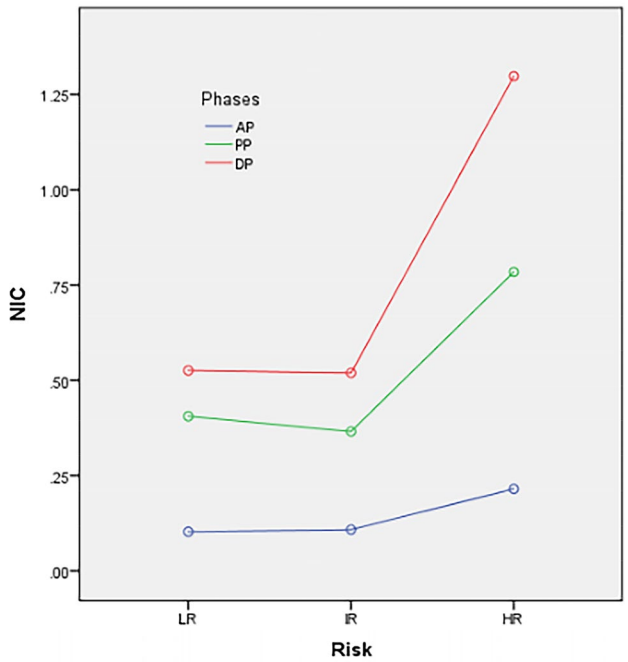

Fig. 7 The NIC values with different risks in different phases. A more delayed phase with higher NIC values in each risk stratification of GIST

the variation of the material CT value with the energy of the X-ray and absorption characteristics relative to different X-ray energies. Various substances exhibit changes in chemical molecular structures, and different chemical molecules have modified energy attenuation curves [11]. Thus, we can distinguish the chemical compositions of substances by comparing the slopes of the spectral curve [17]. The slope is also a measure of the change in CT values, in which the results showed that the slope of the energy spectral curve was higher than that of the non-high-risk group in each phase of enhanced scanning. These results indicate that the CT value of patients with high risk changed significantly. These findings also correlated to the abundant blood supply and active mitosis of the tumor cell.

Iodine concentration provides a more accurate evaluation of the change in CT value after contrast enhancement with an iodine contrast agent. Our study showed that with a delay in scanning time, the iodine concentration of each risk degree GIST increased, which is consistent with GIST progressive enhancement. The NIC value of high-risk GIST is still higher than that of the non-high-risk group. A study performed by Kamiyama et al. [6] suggested that more FDG uptake of the lesion was observed with enhanced malignant potential, and the uptake of FDG was correlated with the Ki-67 index and mitotic values. These findings indicate that glucose metabolism is increased in cells undergoing fission, and the blood requirement and iodine deposition also correspondingly increased. Thus, the iodine concentration can reflect the nature and metabolism of the lesion more accurately.

However, our study had some limitations. First, the study sample size was small, and the results were preliminary, which requires further confirmation by additional studies performed with a larger number of lesions. Second, this study focused on the risk classification of GIST. The correlation between the type of GIST mutations and risk remains to be further investigated.

In summary, predicting the recurrence risk of gastrointestinal stromal tumors with quantitative imaging parameters is only a preoperative evaluation method and cannot completely replace histopathological examination. However, if the risk degree is accurately judged before surgery, surgical trauma of some patients can be avoided, or surgical opportunities can be obtained after drug treatment. Therefore, preoperative evaluation is particularly important. GIST could be classified as high risk and non-high risk with dual-energy spectral CT quantitative parameters, such as CT value of 70 keV monochromatic images, the slope of spectral curves, and the normalized iodine concentration (NIC). Our results should be validated with a larger prospective study using a different agent to assess if these findings are generalizable.

Acknowledgements This research was supported by the Talent Innovation and Entrepreneurship Project of Lanzhou: Project Name—Application value and technological innovation of dual-energy spectral CT in thoracic and abdominal tumor (No. 2016-RC-58).

Compliance with ethical standards

Conflict of interest The authors declare no potential conflicts of interest.

Ethical approval All procedures performed in studies involving human participants were in accordance with the ethical standards of the institutional research committee and with the 1964 Helsinki declaration and its later amendments or comparable ethical standards.

Informed consent Informed consent was obtained from all individual participants included in the study.

References

1. H. Joensuu. Risk stratification of patients diagnosed with gastrointestinal stromal tumor[J]. Hum Pathol, 2008,39(10):1411-9.
2. A. C. O'Neill, A. B. Shinagare, V. Kurra, et al. Assessment of metastatic risk of gastric GIST based on treatment-naive CT features[J]. Eur J Surg Oncol, 2016,42(8):1222-8.
3. S. H. Tirumani, A. D. Baheti, H. Tirumani, et al. Update on Gastrointestinal Stromal Tumors for Radiologists[J]. Korean J Radiol, 2017,18(1):84-93.
4. A. Dimitrakopoulou-Strauss, U. Ronellenfitsch, C. Cheng, et al. Imaging therapy response of gastrointestinal stromal tumors (GIST) with FDG PET, CT and MRI: a systematic review[J]. Clin Transl Imaging, 2017,5(3):183-197.
5. A. B. Shinagare, I. K. Ip, R. Lacson, et al. Gastrointestinal stromal tumor: optimizing the use of cross-sectional chest imaging during follow-up[J]. Radiology, 2015,274(2):395-404.
6. Z. Pan, L. Pang, B. Ding, et al. Gastric cancer staging with dual energy spectral CT imaging[J]. PLoS One, 2013,8(2):e53651.
7. L. Consolino, D. L. Longo, M. Sciortino, et al. Assessing tumor vascularization as a potential biomarker of imatinib resistance in gastrointestinal stromal tumors by dynamic contrast-enhanced magnetic resonance imaging[J]. Gastric Cancer, 2017,20(4):629-639.
8. Y. Kamiyama, R. Aihara, T. Nakabayashi, et al. 18F-fluorodeoxyglucose positron emission tomography: useful technique for predicting malignant potential of gastrointestinal stromal tumors[J]. World J Surg, 2005,29(11):1429-35.
9. M. H. Yu, J. M. Lee, J. H. Baek, et al. MRI features of gastrointestinal stromal tumors[J]. AJR Am J Roentgenol, 2014,203(5):980-91.
10. A. Nowain, H. Bhakta, S. Pais, et al. Gastrointestinal stromal tumors: clinical profile, pathogenesis, treatment strategies and prognosis[J]. J Gastroenterol Hepatol, 2005,20(6):818-24.
11. M. Karcaaltincaba, A. Aktas. Dual-energy CT revisited with multidetector CT: review of principles and clinical applications[J]. Diagn Interv Radiol, 2011,17(3):181-94.
12. C. H. McCollough, S. Leng, L. Yu, et al. Dual- and Multi-Energy CT: Principles, Technical Approaches, and Clinical Applications[J]. Radiology, 2015,276(3):637-53.
13. C. L. Corless, J. A. Fletcher,M. C. Heinrich. Biology of gastrointestinal stromal tumors[J]. J Clin Oncol, 2004,22(18):3813-25.
14. M. Jinzaki, A. Tanimoto, M. Mukai, et al. Double-phase helical CT of small renal parenchymal neoplasms: correlation with pathologic findings and tumor angiogenesis[J]. J Comput Assist Tomogr, 2000,24(6):835-42.
15. D. M. McDonald,P. Baluk. Significance of blood vessel leakiness in cancer[J]. Cancer Res, 2002,62(18):5381-5.
16. V. E. Reuter. The pathology of renal epithelial neoplasms[J]. Semin Oncol, 2006,33(5):534-43.
17. A. Graser, T. R. Johnson, H. Chandarana, et al. Dual energy CT: preliminary observations and potential clinical applications in the abdomen[J]. Eur Radiol, 2009,19(1):13-23.